Supporting Information

Hierarchical N/S co-doped carbon anodes fabricated through facile ionothermal polymerization for high-performance sodium ion batteries

Wenlong Shao,[a] Fangyuan Hu,[b,*] Ce Song,[c] Jinyan Wang,[a] Cheng Liu,[a] Zhihuan Weng,[a] Xigao Jian[a,b,c,*]

[a] *State Key Laboratory of Fine Chemicals, Liaoning Province Engineering Research Centre of High Performance Resins. Dalian University of Technology, Dalian, 116024, China. *E-mail: hufangyuan@dlut.edu.cn*

[b] *School of Materials Science and Engineering, State Key Laboratory of Fine Chemicals, Liaoning Province Engineering Centre of High Performance Resins. Dalian University of Technology, Dalian 116024, China.*

[c] *School of Mathematical Sciences, Dalian University of Technology, Dalian 116024, China.*

Table of content

1. Experimental section.

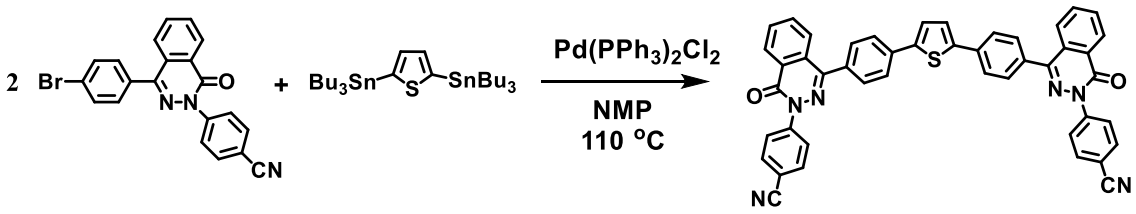

PHPZ-CN **STPN**

Synthesis of monomers and polymers:

Compound **PHPZ-CN** and **2,5-bis(tributylstannyl)thiophene** were synthesized according to the literature.[1-2]

4,4'-((thiophene-2,5-diylbis(4,1-phenylene))bis(1-oxophthalazine-4,2(1H)-diyl))dibenzonitrile (STPN). To a mixture of PHPZ-CN (3.538 g, 8.8 mmol) and 2,5-bis(tributylstannyl)thiophene (2.646 g, 4.0 mmol) in *N*-methyl-2-pyrrolidone (NMP) 30 mL, $PdCl_2(PPh_3)_2$ (0.124 g, 0.18 mmol) was added under a N_2 atmosphere. The mixture was stirred for 42 h under 110 °C. The resulting mixture was poured into water, then a greyish-green precipitate was filtered. The resulting solid was washed with hot NMP, *N,N*-dimethyl acetamide (DMAc) , ethanol and water, and subjected to Soxhlet extraction successively with tetrahydrofuran and ethanol, then dried under vacuum. 1.30 g of faint yellow product was obtained (yield: 44.83%). Calcd for $C_{46}H_{26}N_6O_2S$: 726.1838, ToF MS EI$^+$ found 726.1804. Anal. Calcd for $C_{46}H_{26}N_6O_2S$: C, 76.02; H, 3.61; N, 11.56; S, 4.41. Found: C, 75.84; H, 3.44; N, 11.41; S, 4.77.

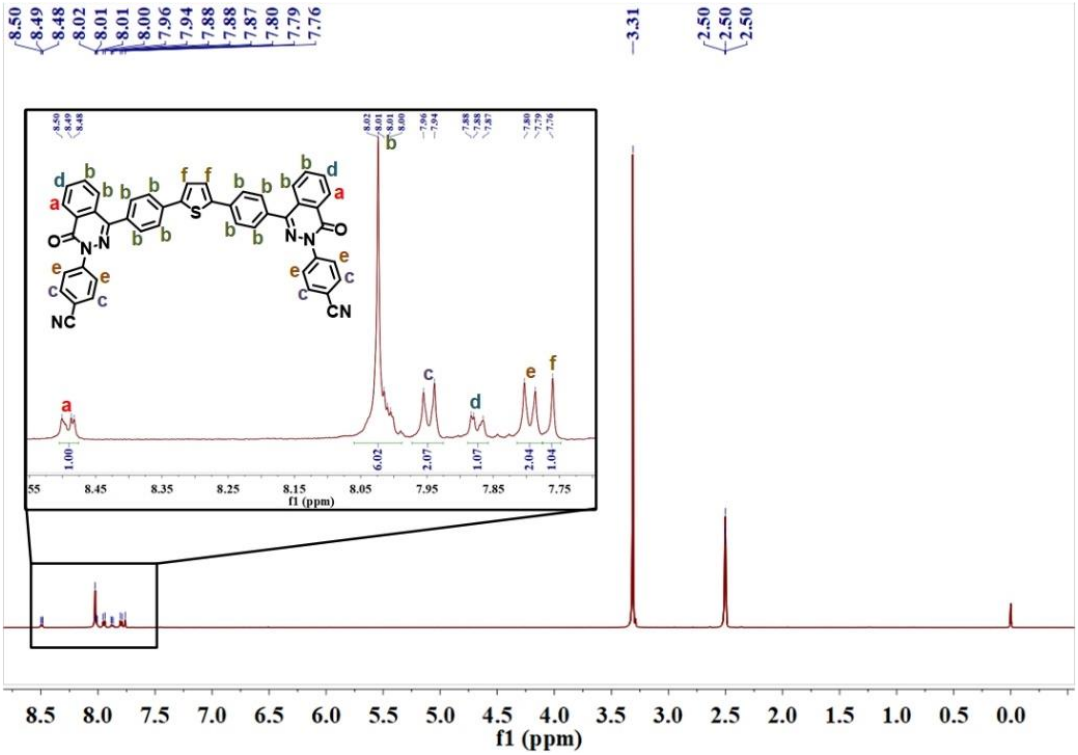

Figure S1. ^{1}H-NMR spectrum of STPN (in DMSO-d^6).

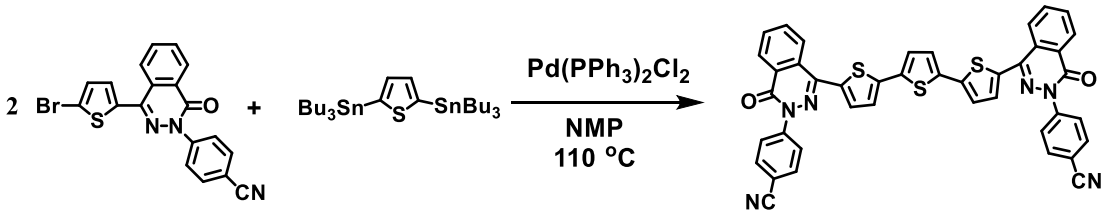

THPZ-CN **TTPN**

Compound **THPZ-CN** was synthesized according to the literature.[1]

4,4'-([2,2':5',2''-terthiophene]-5,5''-diylbis(1-oxophthalazine-4,2(1H)-diyl)) dibenzonitrile (TTPN). To a mixture of THPZ-CN (3.590 g, 8.8 mmol) and 2,5-bis(tributylstannyl)thiophene (2.646 g, 4.0 mmol) in *N*-methyl-2-pyrrolidone (NMP) 30 mL, $PdCl_2(PPh_3)_2$ (0.124 g, 0.18 mmol) was added under a N_2 atmosphere. The mixture was stirred for 42 h under 110 °C. The resulting mixture was poured into water, then a salmon precipitate was filtered. The resulting solid was washed with hot NMP, *N,N*-dimethyl acetamide (DMAc) , ethanol and water, and subjected to Soxhlet extraction successively with tetrahydrofuran and ethanol, then dried under vacuum. 2.15 g of red product was obtained (yield: 72.83%). Calcd for $C_{42}H_{22}N_6O_2S_3$: 738.0966, ToF MS EI^+ found 738.0968. Anal. Calcd for $C_{42}H_{22}N_6O_2S_3$: C, 68.28; H, 3.00; N, 11.37; S, 13.02. Found: C, 62.81; H, 2.82; N, 9.79; S,12.72.

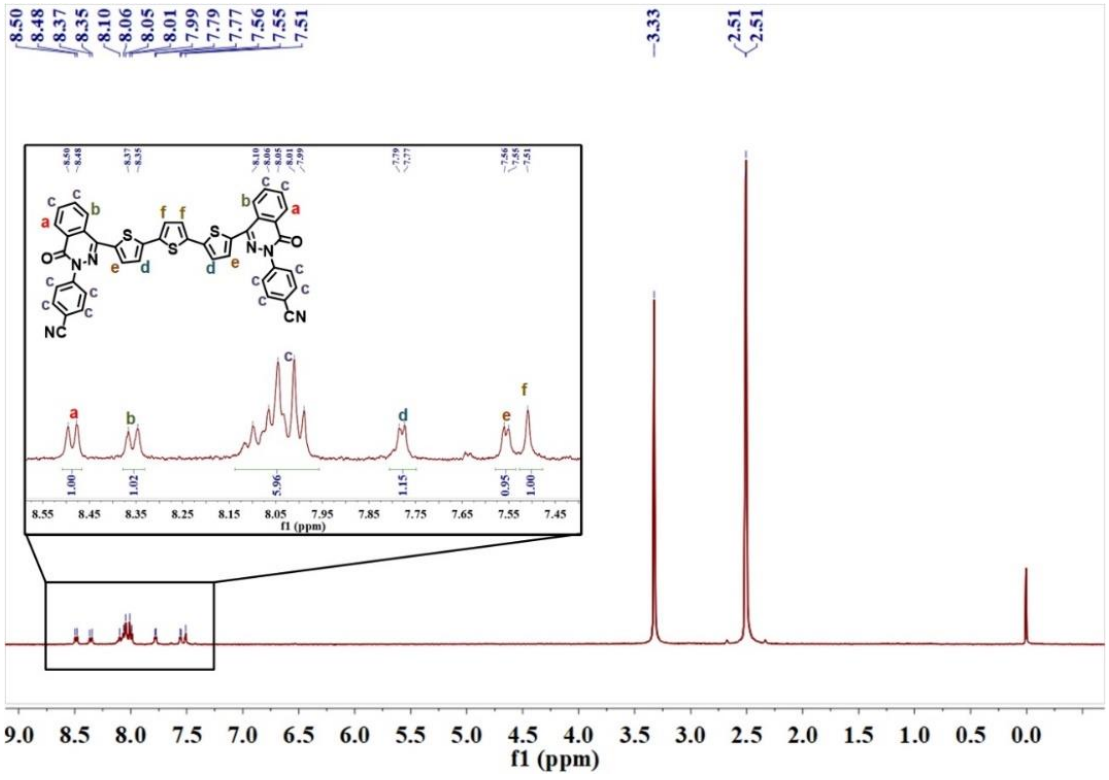

Figure S2. ^{1}H-NMR spectrum of TTPN (in DMSO-d^6).

2. FT-IR spectra and TGA curves of the precursors.

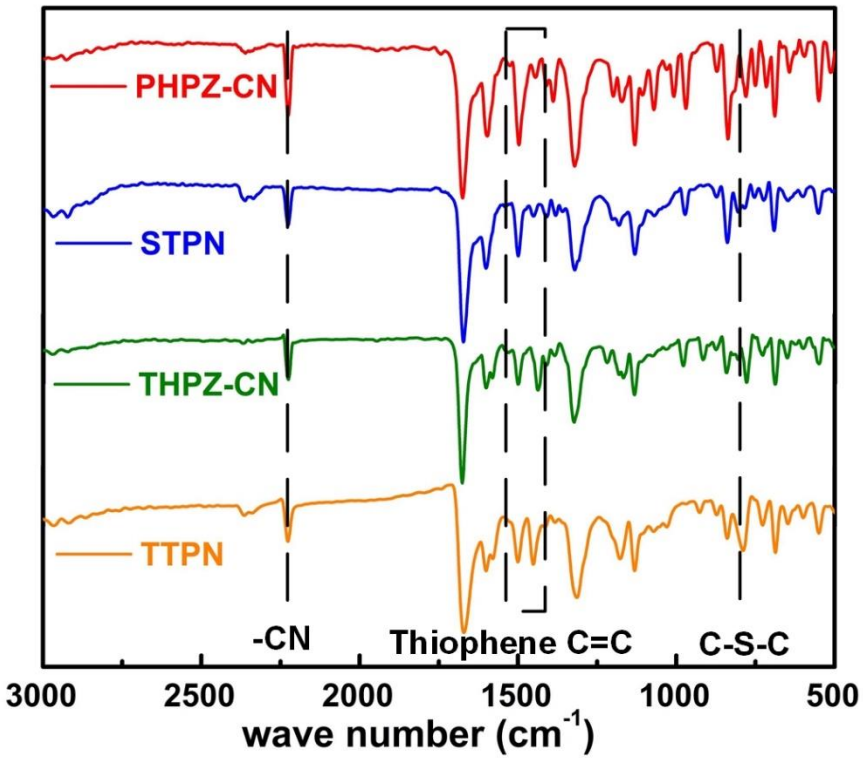

Figure S3. FT-IR spectra of PHPZ-CN, THPZ-CN, STPN, and TTPN.

All the precursors showed the characteristic absorption peak in 2230 cm^{-1}, indicating that –CN existed in all the precursors. Characteristic absorption peak in ~800 cm^{-1} representing the C-S-C bond in thiophene, indicating that the PHPZ-CN transferred into STPN successfully.

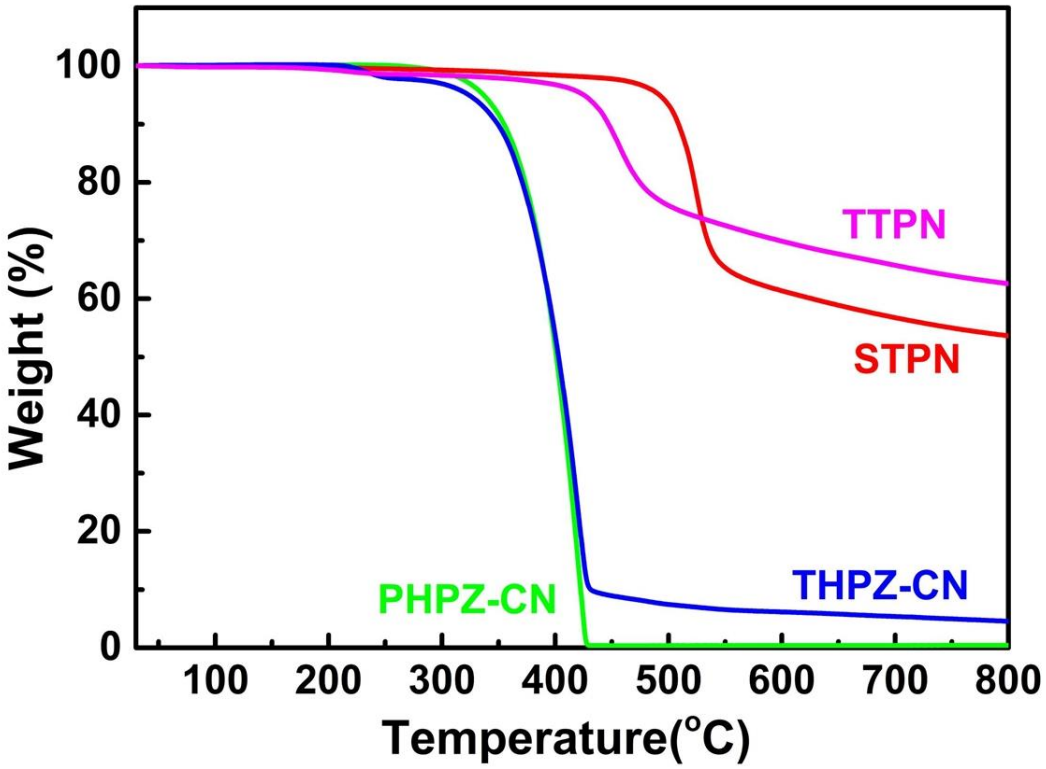

Figure S4. TGA curves of PHPZ-CN, THPZ-CN, STPN, and TTPN.

TGA curves showed that both of STPN and TTPN were going to degrade over 400 °C, the degradation temperature is higher than PHPH-CN and THPZ-CN, indicating the PHPZ-CN and TPHZ-CN transferred into STPN and TTPN successfully after the conversion reaction.

3. SEM, TEM of the products.

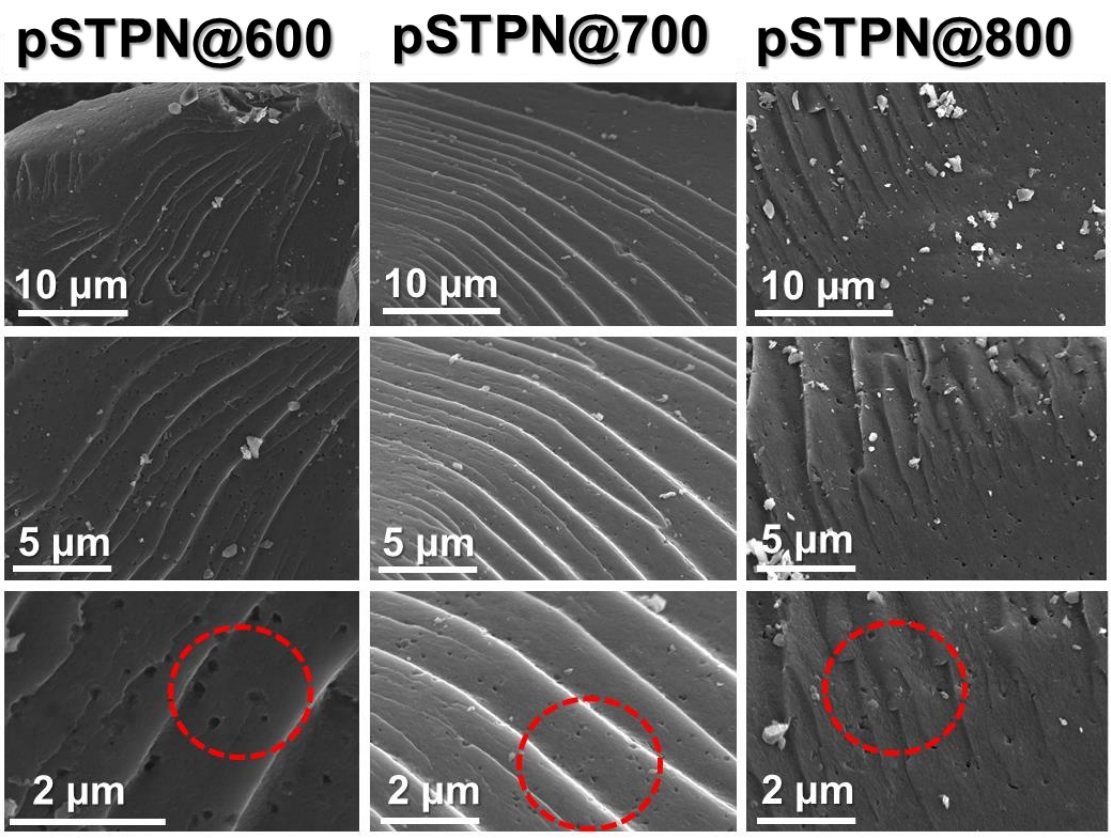

Figure S5. The SEM images of pSTPN@600, pSTPN@700, and pSTPN@800.

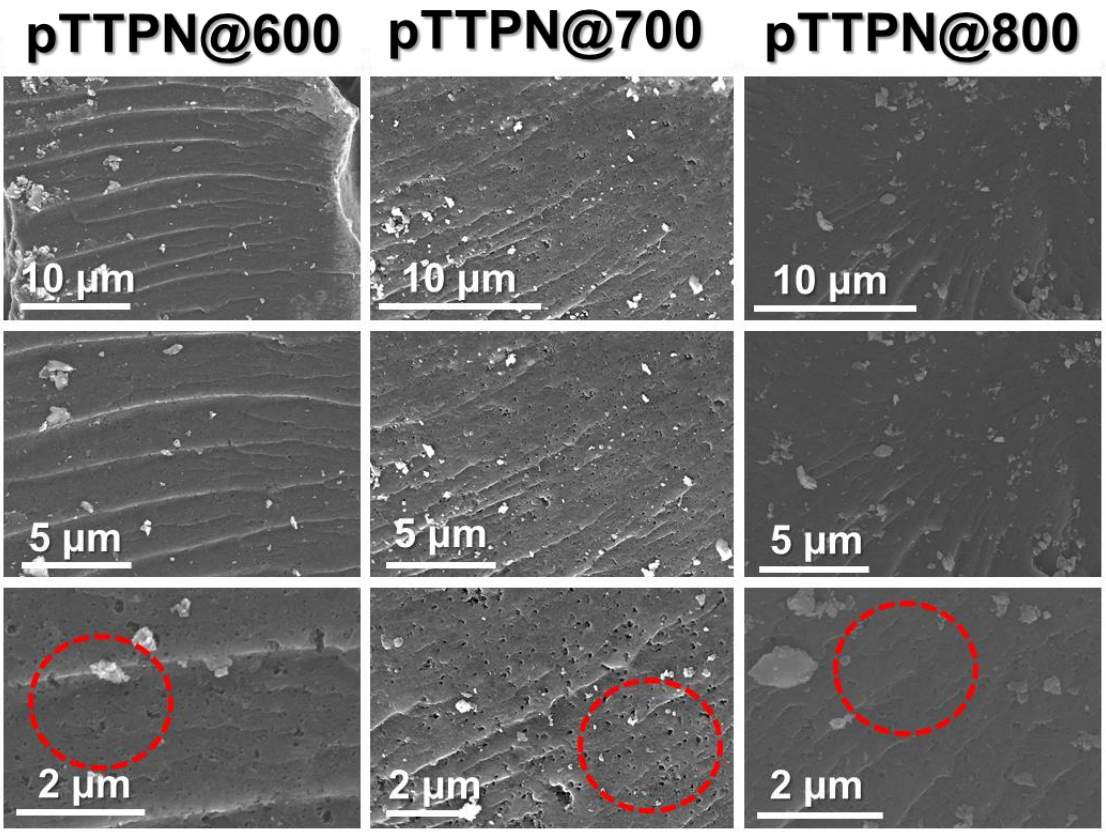

Figure S6. The SEM images of pTTPN@600, pTTPN@700, and pTTPN@800.

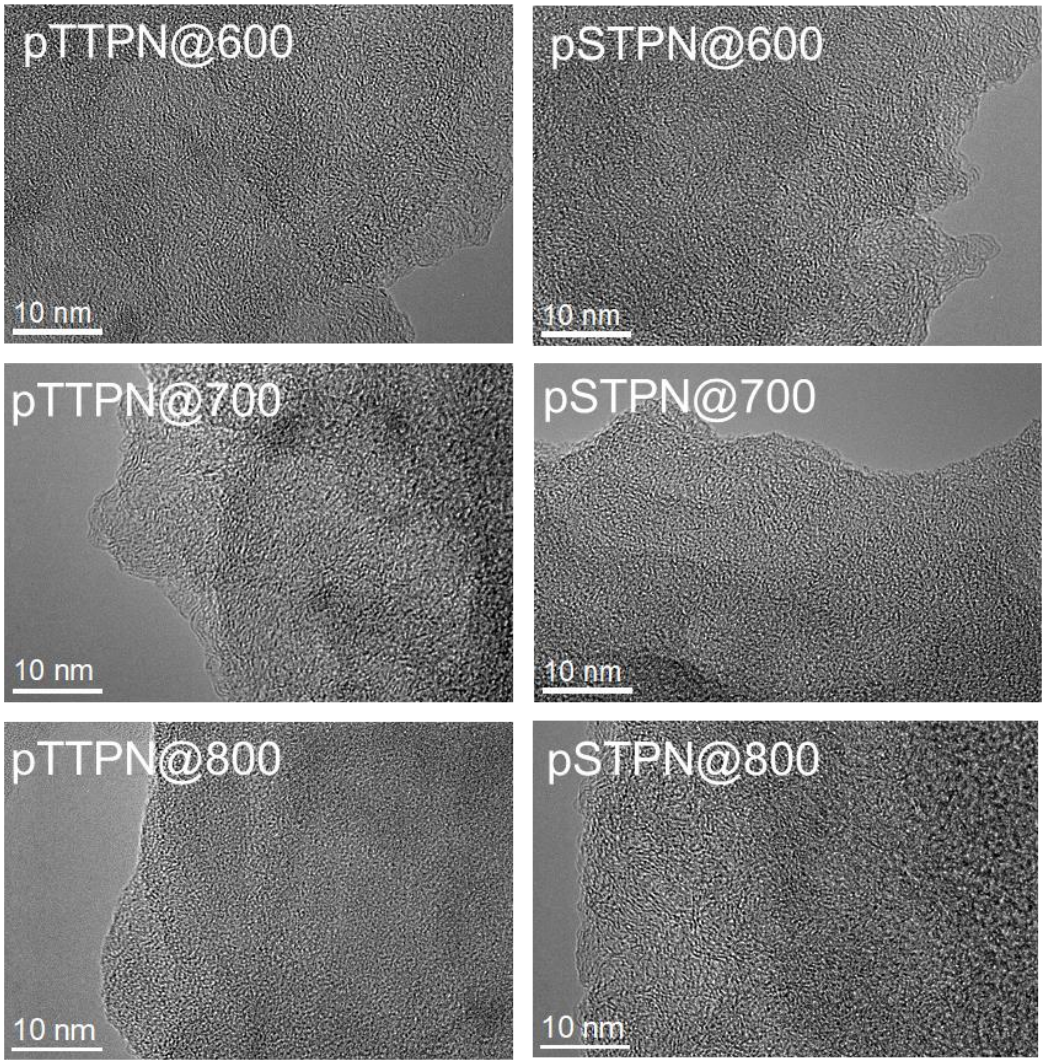

Figure S7. The TEM images of pTTPN@600, pTTPN@700, pTTPN@800, pSTPN@600, pSTPN@700, and pSTPN@800.

4. FT-IR, XRD, and Raman curves of the products.

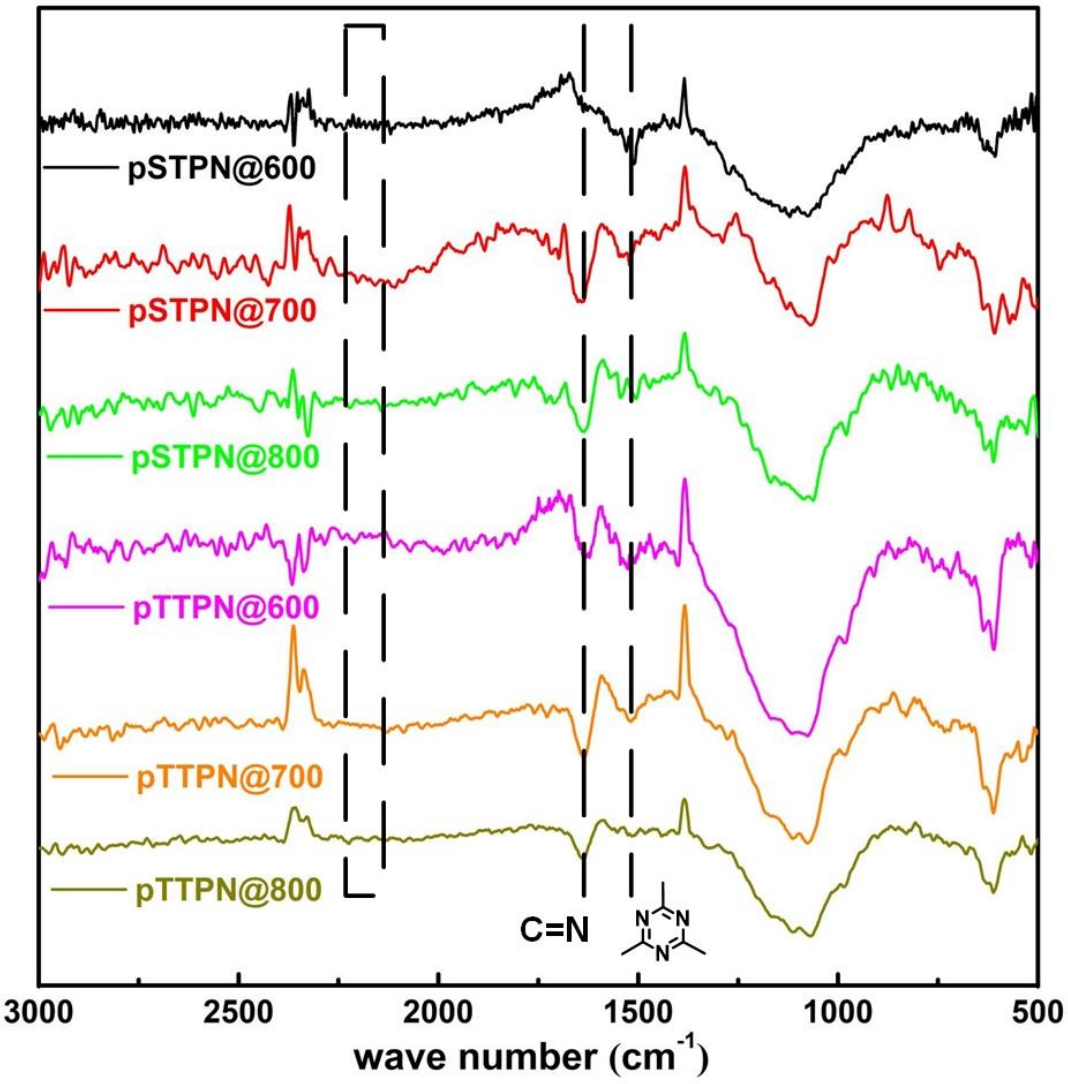

Figure S8. FT-IR spectra of pSTPN@600, pSTPN@700, pSTPN@800, pTTPN@600, pTTPN@700, and pTTPN@800.

Figure S8 showed that characteristic absorption peak of –CN in 2230 cm^{-1} disappeared, and characteristic absorption peak representing the triazine ring appeared after ionothermal reaction, indicating the formation of porous polymer-derived carbon.

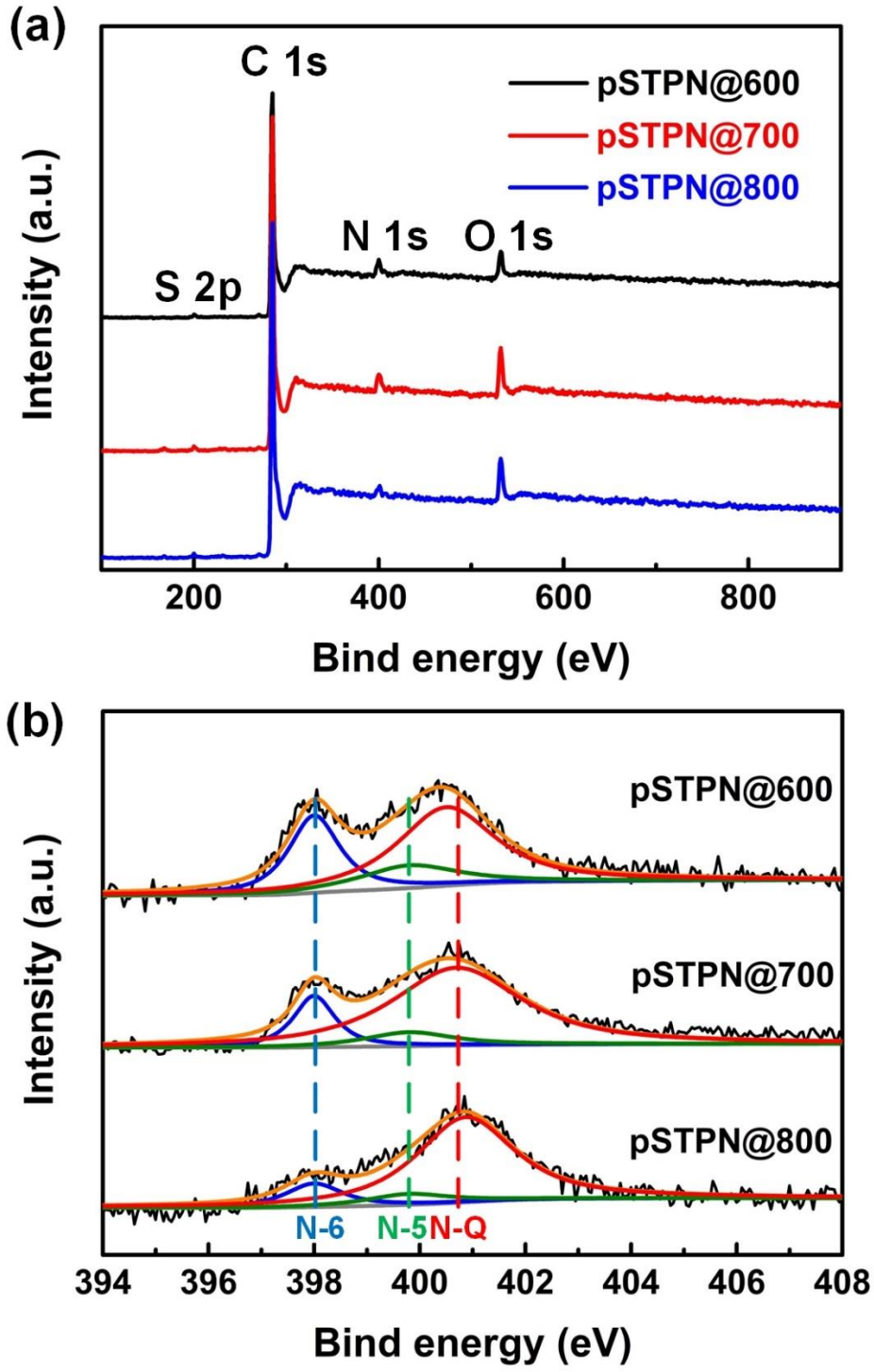

Figure S9. a) X-ray photoelectron spectra (XPS) of pSTPN@600, pSTPN@700, and pSTPN@800. b) High-resolution N 1s XPS spectra of pSTPN@600, pSTPN@700, and pSTPN@800.

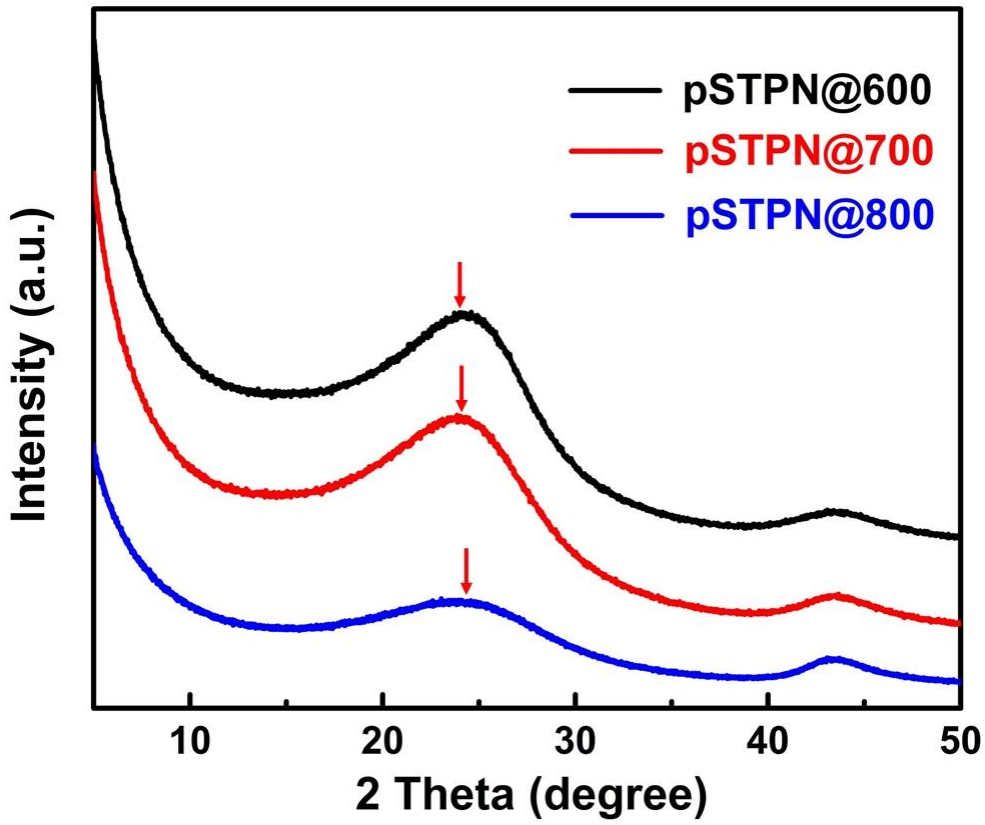

Figure S10. XRD patterns of pSTPN@600, pSTPN@700, and pSTPN@800.

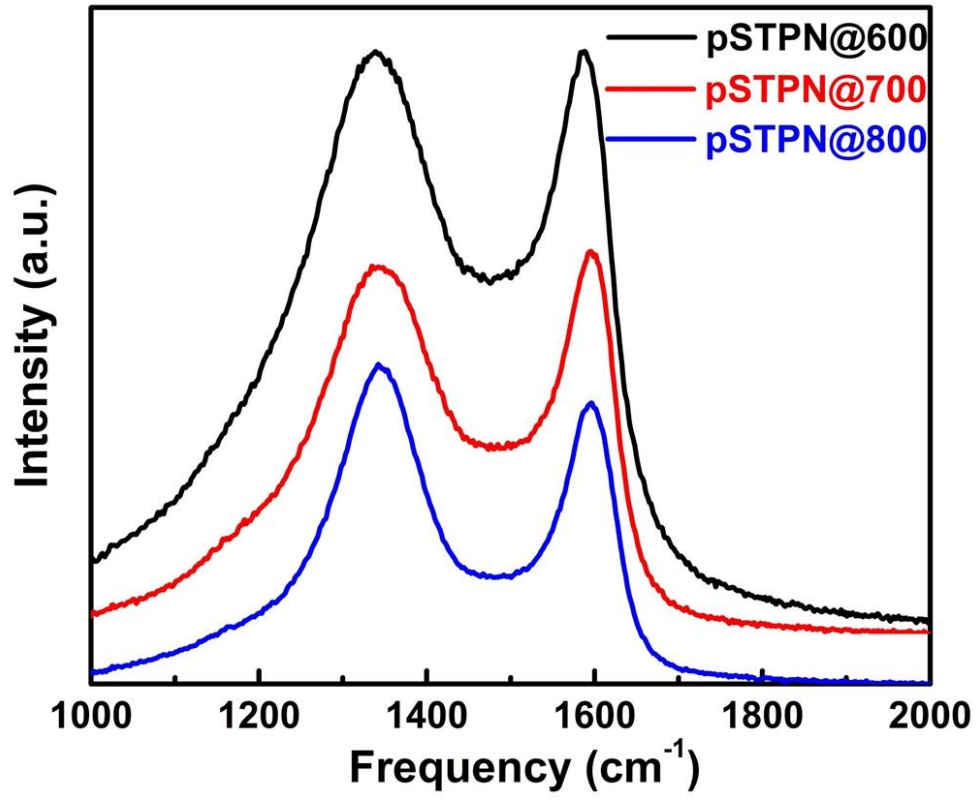

Figure S11. Raman spectra of pSTPN@600, pSTPN@700, and pSTPN@800.

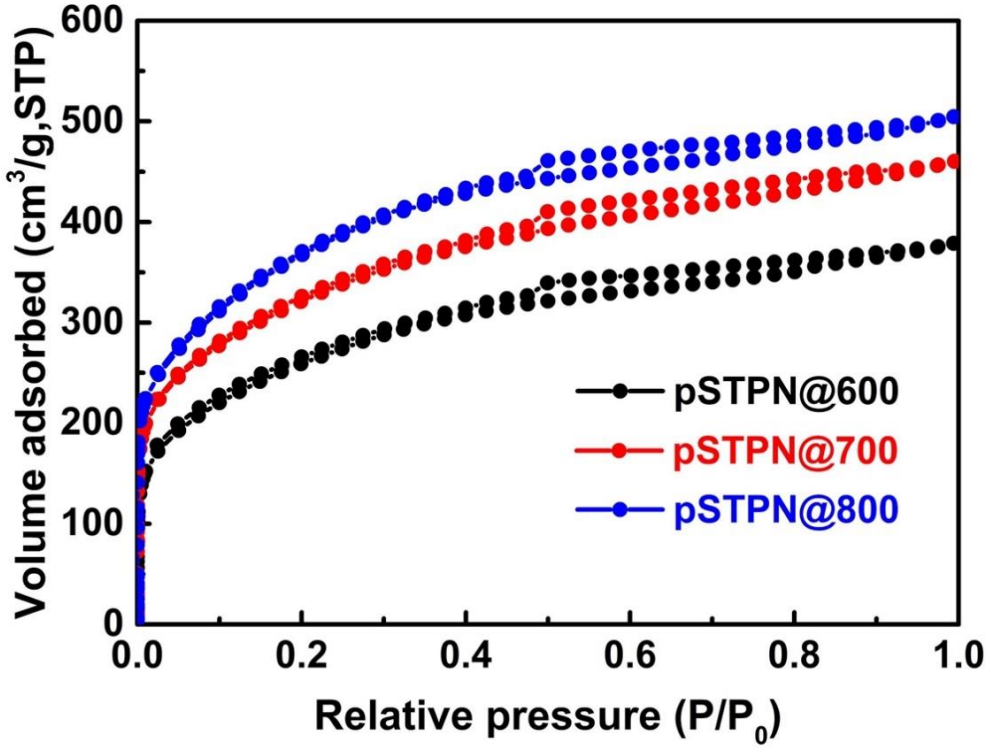

Figure S12. N_2 adsorption-desorption isothermal curves of pSTPN@600, pSTPN@700, and pSTPN@800.

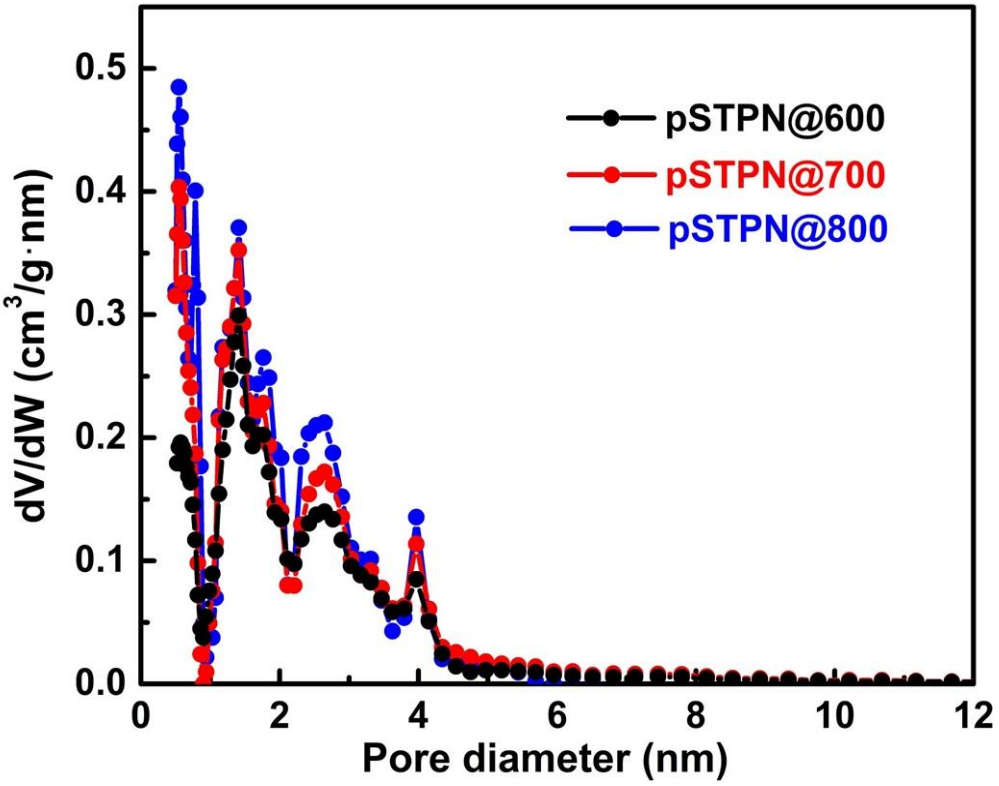

Figure S13. Pore size distribution of pSTPN@600, pSTPN@700, and pSTPN@800 calculated by DFT method.

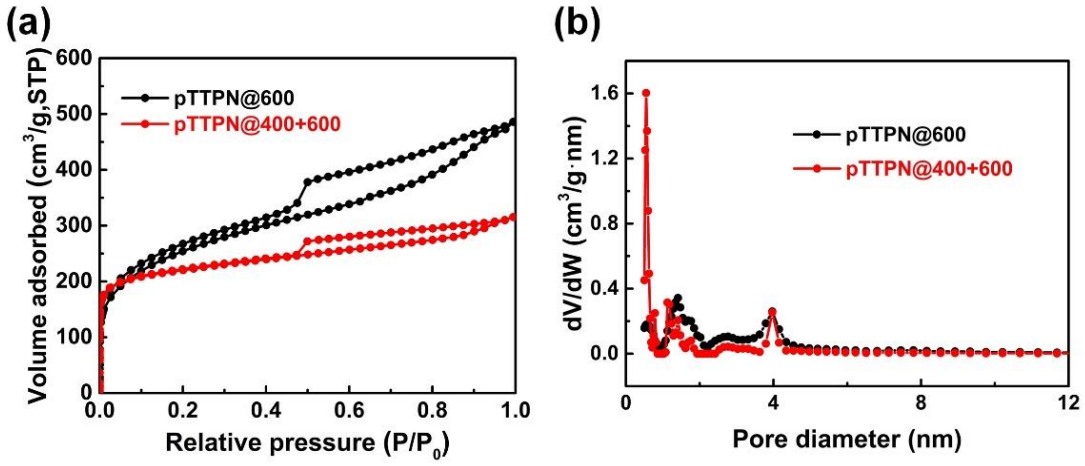

Figure S14. N_2 adsorption-desorption isothermal curves (a) and corresponding pore size distribution (b) of pTTPN@400+600 and pTTPN@600.

5. Electrochemical performance of the products.

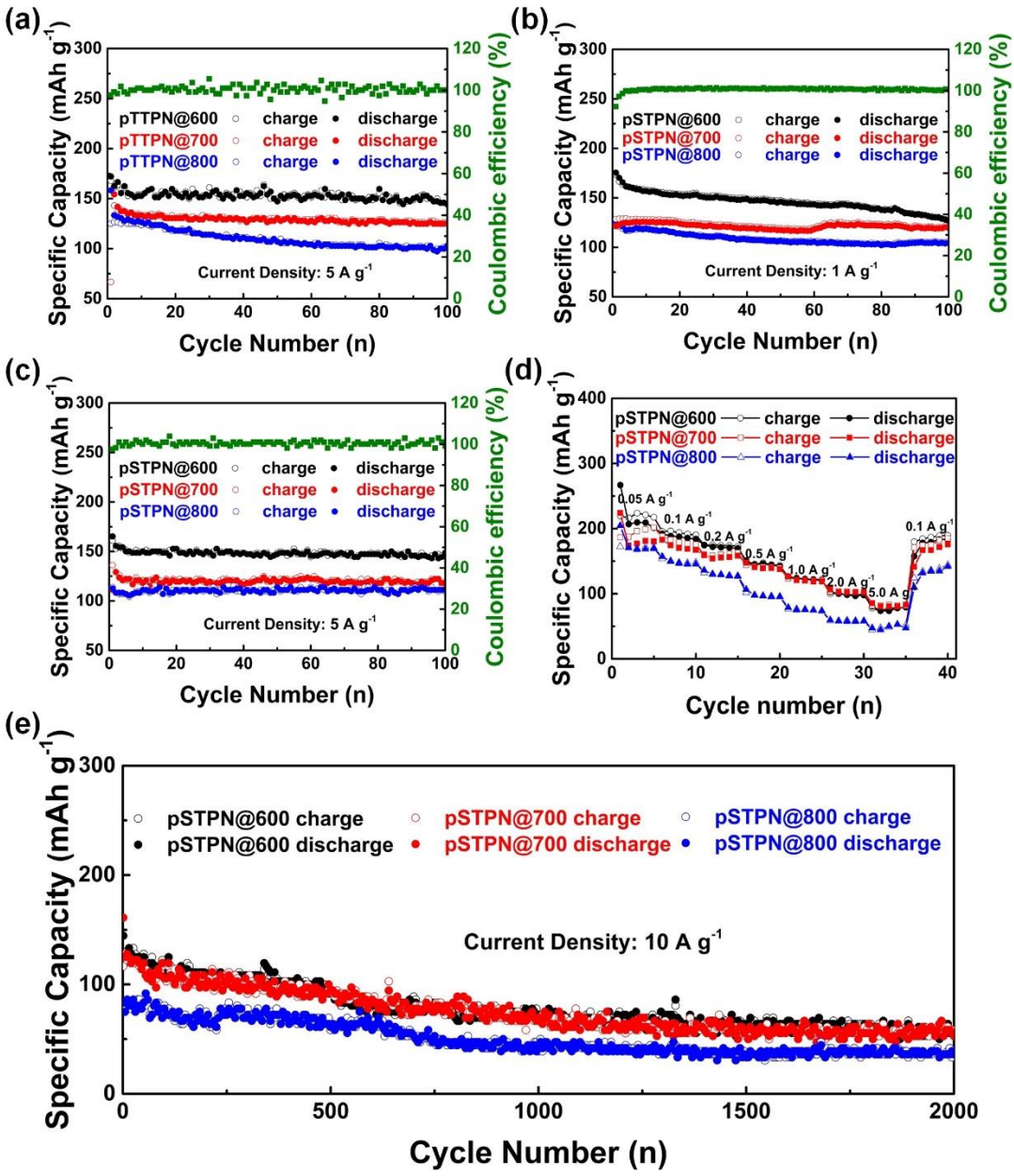

Figure S15. a) Cycling performance of pTTPN@600, pTTPN@700, and pTTPN@800 electrodes at the current density of 5 A g^{-1}. b,c) Cycling performance of pSTPN@600, pSTPN@700, and pSTPN@800 electrodes at the current density of 1 A g^{-1} and 5 A g^{-1}. d) Rate performance of pSTPN@600, pSTPN@700, and pSTPN@800 electrodes at the current densities of 0.05, 0.1, 0.2, 0.5, 1.0, 2.0, and 5.0 A g^{-1}. e) Long cycle performance of pSTPN@600, pSTPN@700, and pSTPN@800 electrodes at the current density of 10 A g^{-1}.

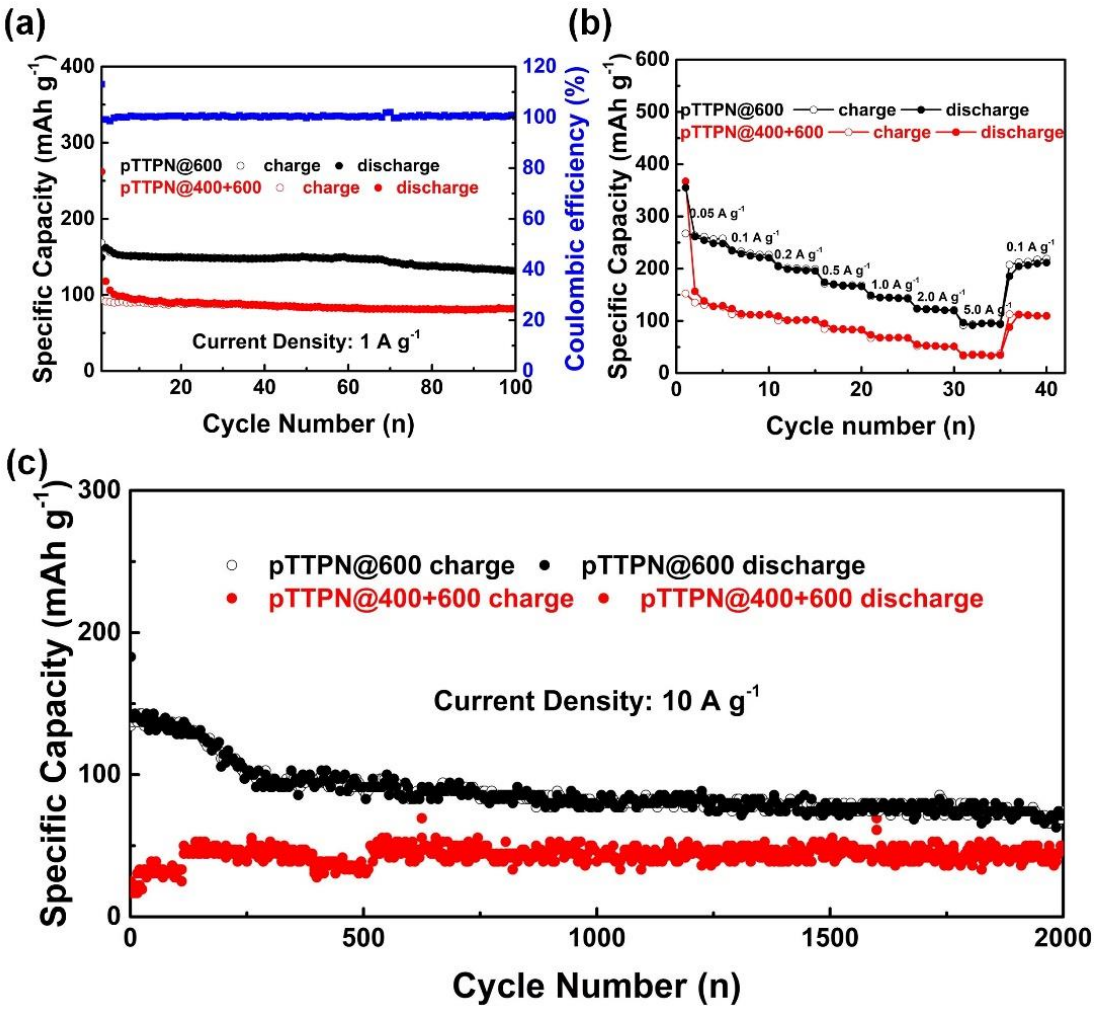

Figure S16. (a) Cycling performance of pTTPN@400+600 and pTTPN@600 at the current density of 1 A g^{-1}. (b) Rate performance of pTTPN@400+600 and pTTPN@600 electrodes at the current densities of 0.05, 0.1, 0.2, 0.5, 1.0, 2.0, and 5.0 A g^{-1}. (c) Long cycle performance of pTTPN@400+600 and pTTPN@600 electrodes at the current density of 10 A g^{-1}.

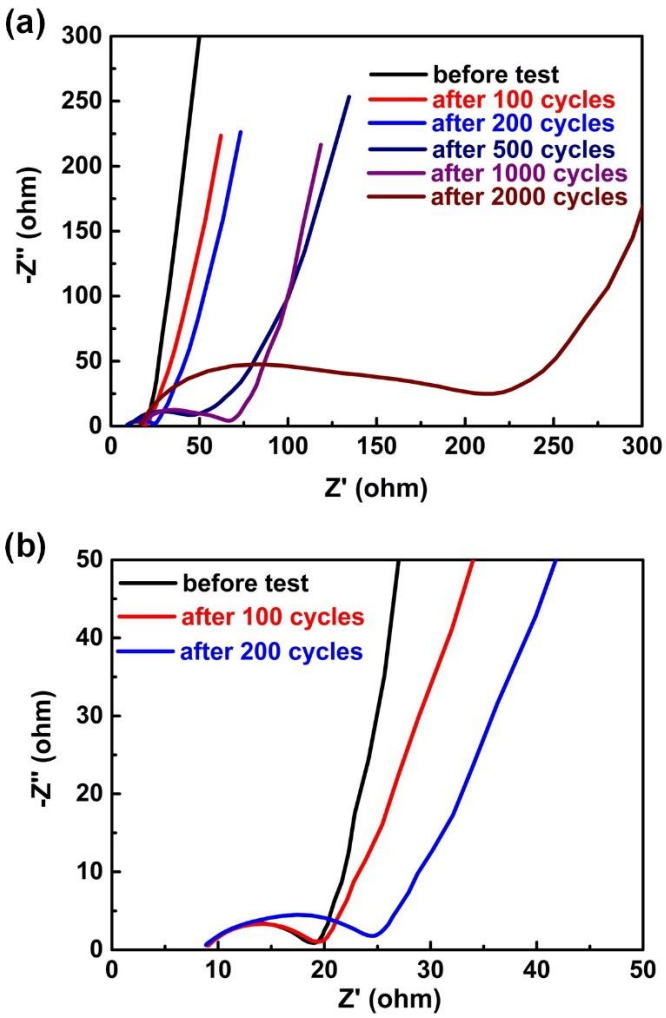

Figure S17. a) Nyquist plots for pTTPN@600 electrode after different cycle numbers. b) Partial enlargement of the Nyquist plots.

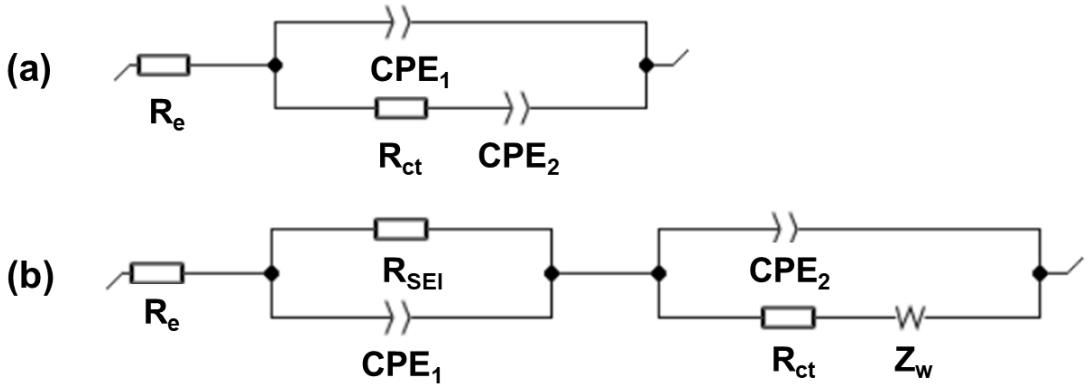

Figure S18. Equivalent circuits used for fitting the EIS plots a) Before test, b) After different cycle numbers.

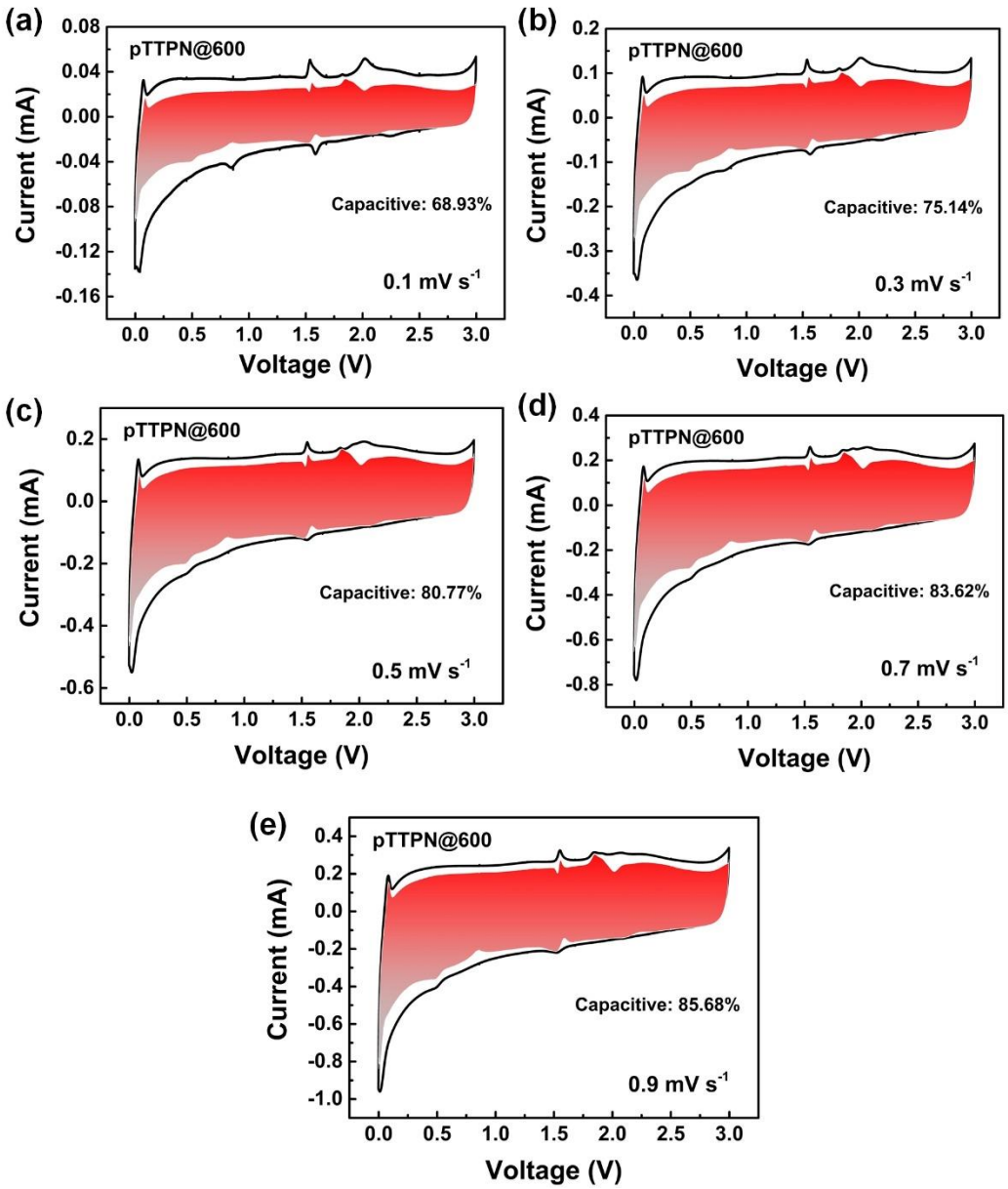

Figure S19. Separation of storage contributions of pTTPN@600 electrode from the capacitance and diffusion-controlled process at various scan rates: a) 0.1mV s^{-1}, b) 0.3mV s^{-1}, c) 0.5mV s^{-1}, d) 0.7mV s^{-1}, and e) 0.9mV s^{-1}.

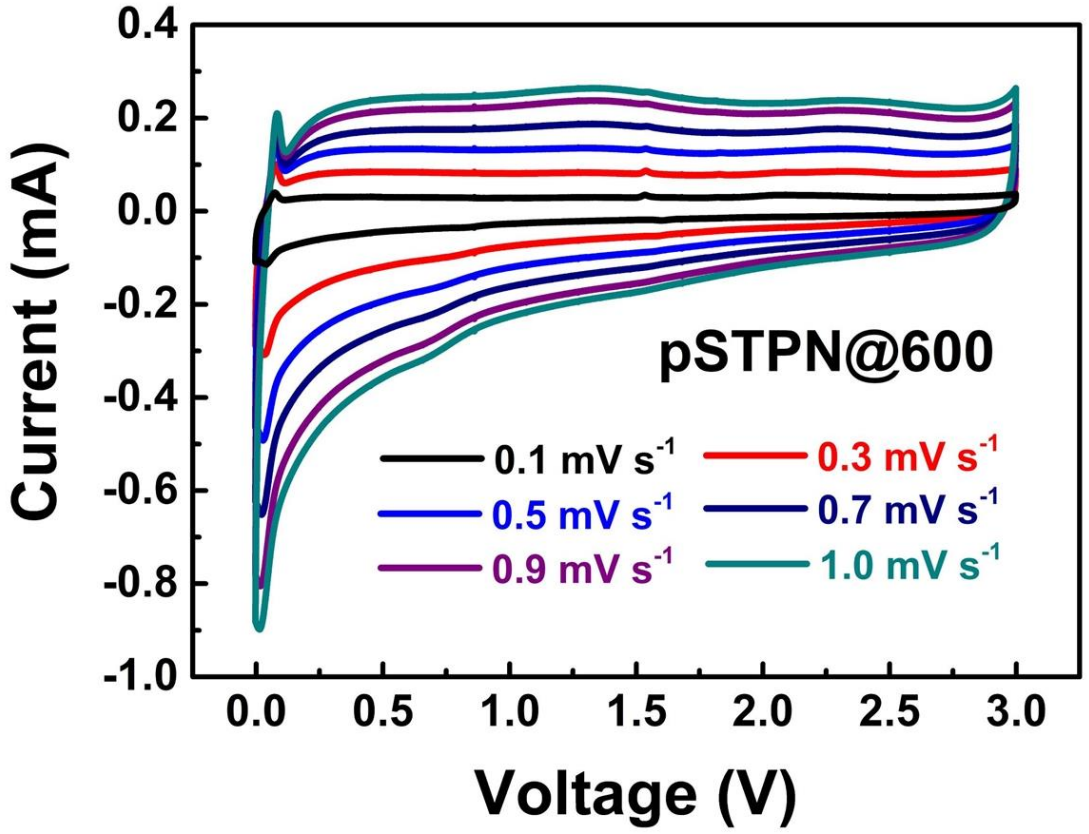

Figure S20. CV curves of pSTPN@600 electrode at different scan rates.

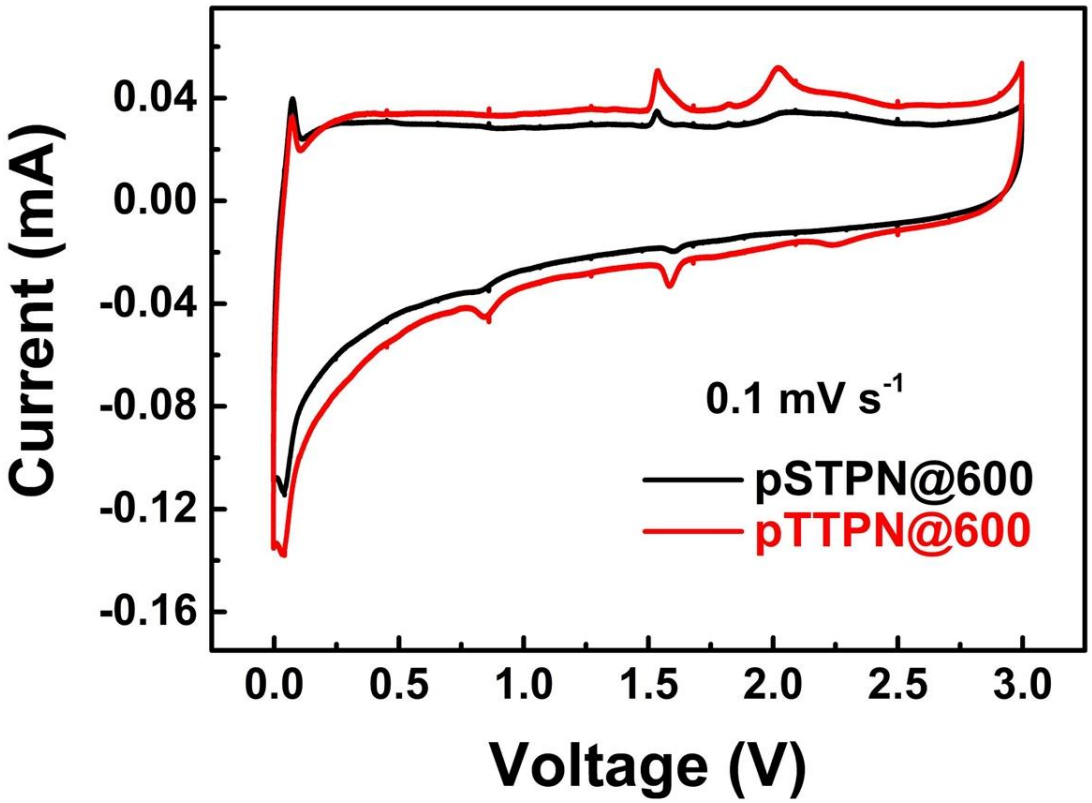

Figure S21. CV curves of the pSTPN@600 and pTTPN@600 electrodes at 0.1 mV s^{-1}.

Table S1. Impedance parameters of pTTPN@600 electrode after different cycling numbers.

pTTPN@600	R_e [a](Ω)	R_{SEI} [b](Ω)	R_{ct} [c](Ω)
prior to cycling	8.58		11.06
after 100 cycles	8.71	10.90	8.61
after 200 cycles	8.85	17.71	15.47
after 500 cycles	8.98	44.40	41.38
after 1000 cycles	15.17	53.49	49.96
after 2000 cycles	16.66	108.8	70.30

[a] R_e: electrolyte resistance.
[b] R_{SEI}: SEI layer resistance.
[c] R_{ct}: changer-transfer resistance.

Table S2. Impedance parameters of the pSTPN@600, pSTPN@700, pSTPN@800, pTTPN@600, pTTPN@700, and pTTPN@800 electrodes.

Sample	R_e [a](Ω)	R_{ct} [b](Ω)	Sample	R_e [a](Ω)	R_{ct} [b](Ω)
pTTPN@600	8.584	11.06	pSTPN@600	9.211	13.60
pTTPN@700	10.69	16.78	pSTPN@700	10.73	149.40
pTTPN@800	8.616	197.70	pSTPN@800	10.97	385.70

[a] R_e: electrolyte resistance.
[b] R_{ct}: changer-transfer resistance.

Table S3 Comparison of electrochemical performances between pTTPN@600 and carbon-based anode materials reported previously.

Anode material	precursor	Rate capability	cyclability	Reference
N-doped carbon sheet	soybean	200 mA h g^{-1} @ 0.3C 150 mA h g^{-1} @ 1.5C 80 mA h g^{-1} @ 4.5C 32.3 mA h g^{-1} @ 30C (1C=375 mA g^{-1})	50 mA h g^{-1} @ 4.5C after 2000 cycles	[3]
Hard carbon microtubes	cotton	310 mA h g^{-1} @ 0.1C 275 mA h g^{-1} @ 0.5C 190 mA h g^{-1} @ 1.0C 80 mA h g^{-1} @ 2.0C (1C=300 mA g^{-1})	305 mA h g^{-1} @ 0.1C after 100 cycles	[4]
Hard carbon	Apple	222 mA h g^{-1} @ 0.2C 181 mA h g^{-1} @ 1C 112 mA h g^{-1} @ 5C 86 mA h g^{-1} @ 10C (1C=200 mA g^{-1})	85 mA h g^{-1} @ 5C after 1000 cycles	[5]
S-doped carbon	PEDOT	327.8 mA h g^{-1} @ 0.5A g^{-1} 242.0 mA h g^{-1} @ 1.0A g^{-1} 192.5 mA h g^{-1} @ 2.0A g^{-1} 119.5 mA h g^{-1} @ 5.0A g^{-1}	302 mA h g^{-1} @ 0.5A g^{-1} after 700cycles	[6]
Graphene-coupled porous carbon	Graphene, CTF	155 mA h g^{-1} @ 0.1A g^{-1} 150 mA h g^{-1} @ 0.5A g^{-1} 140 mA h g^{-1} @ 1.0A g^{-1} 133 mA h g^{-1} @ 5.0A g^{-1}	137 mA h g^{-1} @ 1.0A g^{-1} after 500cycles	[7]
Mesoporous soft carbon	Mesophase pitch	260 mA h g^{-1} @ 0.05A g^{-1} 193 mA h g^{-1} @ 0.1A g^{-1} 105 mA h g^{-1} @ 1.0A g^{-1} 62 mA h g^{-1} @ 5.0A g^{-1}	103 mA h g^{-1} @ 0.5A g^{-1} after 3000cycles	[8]
Porous carbon	Carbon black	196 mA h g^{-1} @ 0.1A g^{-1} 159 mA h g^{-1} @ 0.4A g^{-1} 133 mA h g^{-1} @ 1.6A g^{-1} 120 mA h g^{-1} @ 3.2A g^{-1}	72 mA h g^{-1} @ 3.2 A g^{-1} after 2000cycles	[9]
Hard carbon	loofah	300 mA h g^{-1} @ 0.5C 260 mA h g^{-1} @ 1.0 C 217 mA h g^{-1} @ 3.0C 60 mA h g^{-1} @ 20C (1C=300 mA g^{-1})	74 mA h g^{-1} @ 2.1 A g^{-1} after 2000cycles	[10]
2D N-doped carbon nanosheets	Zn-HMT MOF	294 mA h g^{-1} @ 0.2A g^{-1} 274 mA h g^{-1} @ 0.5A g^{-1} 245 mA h g^{-1} @ 1.0A g^{-1} 215 mA h g^{-1} @ 5.0A g^{-1}	170 mA h g^{-1} @ 5.0 A g^{-1} after 1000cycles	[11]

Shell-like N,S co-doped thin carbon	MoF/PVP	372mA h g^{-1} @ 0.5A g^{-1} 316 mA h g^{-1} @ 1.0A g^{-1} 239 mA h g^{-1} @ 8.0A g^{-1} 169 mA h g^{-1} @ 32A g^{-1}	2000 mA h g^{-1} @ 16 A g^{-1} after 4500cycles	[12]
3D Framework Carbon	Sodium Citrate	400 mA h g^{-1} @ 0.1A g^{-1} 278 mA h g^{-1} @ 0.5A g^{-1} 200 mA h g^{-1} @ 1.0A g^{-1} 105 mA h g^{-1} @ 5.0A g^{-1}	99 mA h g^{-1} @ 10 A g^{-1} after 10000cycles	[13]
CQDs transformed 3DCFs	NaOH/ ethanol	208 mA h g^{-1} @ 0.1A g^{-1} 127 mA h g^{-1} @ 1.0A g^{-1} 93 mA h g^{-1} @ 5.0A g^{-1}	87 mA h g^{-1} @ 10.0A g^{-1} after 6500cycles	[14]
3D macroporous structure	GO/NCL	247 mA h g^{-1} @ 0.5A g^{-1} 219 mA h g^{-1} @ 1.0A g^{-1} 90 mA h g^{-1} @ 10.0A g^{-1}	257 mA h g^{-1} @ 0.5A g^{-1} after 2500cycles	[15]
hierarchical N-doped porous carbon	Water hyacinths	248 mA h g^{-1} @ 0.05A g^{-1} 217 mA h g^{-1} @ 0.1A g^{-1} 141 mA h g^{-1} @ 0.8A g^{-1} 120 mA h g^{-1} @ 1.6A g^{-1}	140 mA h g^{-1} @ 0.4A g^{-1} after 1000cycles	[16]
Hierarchical porous carbon	**Porous polymer**	**248 mA h g^{-1} @ 0.05A g^{-1} 224 mA h g^{-1} @ 0.1A g^{-1} 134 mA h g^{-1} @ 1.0A g^{-1} 95 mA h g^{-1} @ 5.0A g^{-1}**	**74 mA h g^{-1} @ 10.0A g^{-1} after 2000cycles**	**This work**

References:

[1] K. Yuan, C. Liu, J. Han, G. Yu, J. Wang, H. Duan, Z. Wang, X. Jian, *RSC Adv.*, 2016, **6**, 12009-12020.

[2] J. Han, K. Yuan, C. Liu, J. Wang, X. Jian, *RSC Adv*., 2015, **5**, 30445-30455.

[3] T. Yang, T. Qian, M. Wang, X. Shen, N. Xu, Z. Sun, C. Yan, *Adv. Mater*. 2016, **28**, 539-545.

[4] Y. Li, Y.S. Hu, M.M. Titirici, L. Chen, X. Huang, *Adv. Energy Mater.,* 2016, **6**, 1600659.

[5] L. Wu, D. Buchholz, C. Vaalma, G. A. Giffin, S. Passerini, *ChemElectroChem*, 2016, **3**, 292-298.

[6] L. Qie, W. Chen, X. Xiong, C. Hu, F. Zou, P. Hu, Y. Huang, *Adv Sci*, 2015, **2**, 1500195.

[7] J. Zhu, X. Zhuang, J. Yang, X. Feng, S.i. Hirano, *J. Mater. Chem. A*, 2017, **5**, 16732-16739.

[8] B. Cao, H. Liu, B. Xu, Y. Lei, X. Chen, H. Song, *J. Mater. Chem. A*, 2016, **4**, 6472-6478.

[9] W. Xiao, Q. Sun, J. Liu, B. Xiao, P.A. Glans, J. Li, R. Li, J. Guo, W. Yang, T.K. Sham, X. Sun, *Nano Res.*, 2017, **10**, 4378-4387.

[10] Y.-E. Zhu, L. Yang, X. Zhou, F. Li, J. Wei, Z. Zhou, *J. Mater. Chem. A,* 2017, **5**, 9528-9532.

[11] S. Liu, J. Zhou, H. Song, *Adv. Energy Mater.,* 2018, **8**, 1800569.

[12] A. Mahmood, S. Li, Z. Ali, H. Tabassum, B. Zhu, Z. Liang, W. Meng, W. Aftab, W. Guo, H. Zhang, M. Yousaf, S. Gao, R. Zou, Y. Zhao, *Adv. Mater*., 2019, **31**, 1805430.

[13] B. Yang, J. Chen, S. Lei, R. Guo, H. Li, S. Shi, X. Yan, *Adv. Energy Mater.,* 2018, **8**, 1702409.

[14] P. Wang, B. Yang, G. Zhang, L. Zhang, H. Jiao, J. Chen, X. Yan, *Chem. Eng. J.,* 2018, **353**, 453-459.

[15] B. Chang, J. Chen, M. Zhou, X. Zhang, W. Wei, B. Dai, S. Han, Y. Huang, *Chem Asian J.*, 2018, **13**, 3859-3864.

[16] G. Zeng, B. Zhou, L. Yi, H. Li, X. Hu, Y. Li. *Sustainable Energy Fuels*. 2018, **2**, 855-861.